AD_____

REPORT NO. T18-90

QUANTIFICATION OF LOWER BOUNDS FOR ENDURANCE TIMES IN THERMALLY INSULATED FINGERS AND TOES EXPOSED TO COLD STRESS

U S ARMY RESEARCH INSTITUTE

OF

ENVIRONMENTAL MEDICINE

Natick, Massachusetts

AUGUST 1990

AD-A227 782

DTIC
ELECTE
OCT 15 1990
D

UNITED STATES ARMY
MEDICAL RESEARCH & DEVELOPMENT COMMAND

The findings in this report are not to be construed as an official Department of the Army position, unless so designated by other authorized documents.

SECURITY CLASSIFICATION OF THIS PAGE

REPORT DOCUMENTATION PAGE		Form Approved OMB No 0704-0188

1a REPORT SECURITY CLASSIFICATION Unclassified	1b RESTRICTIVE MARKINGS

2a SECURITY CLASSIFICATION AUTHORITY	3 DISTRIBUTION/AVAILABILITY OF REPORT Approved for public release; distribution is unlimited
2b DECLASSIFICATION/DOWNGRADING SCHEDULE	

4 PERFORMING ORGANIZATION REPORT NUMBER(S)	5 MONITORING ORGANIZATION REPORT NUMBER(S)

6a NAME OF PERFORMING ORGANIZATION U.S. Army Rsch Inst of Env Med	6b OFFICE SYMBOL (If applicable) SGRD-UE-ME	7a NAME OF MONITORING ORGANIZATION U. S Army Rsch Inst of Env Med

6c. ADDRESS (City, State, and ZIP Code) Natick, MA 01760-5007	7b ADDRESS (City, State, and ZIP Code) Natick, MA 01760-5007

8a NAME OF FUNDING/SPONSORING ORGANIZATION same as 6a.	8b OFFICE SYMBOL (If applicable)	9 PROCUREMENT INSTRUMENT IDENTIFICATION NUMBER

8c. ADDRESS (City, State, and ZIP Code) same as 6c.	10 SOURCE OF FUNDING NUMBERS			
	PROGRAM ELEMENT NO 3E162787A878	PROJECT NO 612787 .878	TASK NO 878/AE	WORK UNIT ACCESSION NO 084

11 TITLE (Include Security Classification) (U) Quantificaton of Lower Bounds for Endurance Times in Thermally Insulated Fingers and Toes Exposed to Cold Stress

12 PERSONAL AUTHOR(S) Avraham Shitzer, Leander A. Stroschein, William R. Santee, Richard R. Gonzales and Kent B. Pandolf

13a TYPE OF REPORT Technical Report	13b TIME COVERED FROM_____ TO_____	14 DATE OF REPORT (Year, Month, Day) July 1990	15 PAGE COUNT 43

16 SUPPLEMENTARY NOTATION

17. COSATI CODES			18 SUBJECT TERMS (Continue on reverse if necessary and identify by block number) analytical model; cold exposure; endurance time; fingers and toes; thermal insulating gloves
FIELD	GROUP	SUB-GROUP	

19 ABSTRACT (Continue on reverse if necessary and identify by block number)
A one-dimensional, analytical solution of axial temperature variations of a circular cylinder is presented. The cylinder is assumed to depict the behavior of similar elements in the body, e.g., fingers and toes. Thermal and physical properties specified for the model pertained to the modeled entity. Blood perfusion effects are lumped into a volumetric heat generation term. Cold-induced vasodilatation (CIVD) effects were not included in the present analysis. A parametric study of environmental temperatures, thermal insulation applied on the cylinder and length and diameter of the cylinder was performed. Specifically, the effects of these parameters on endurance times, as determined by a drop of cylinder (finger) tip temperature to 5°C, were studied. It was found that the lower the temperature, the longer the finger, and the smaller the diameter thereof - the shorter is the endurance time for the same thermal insulation. Results of the model were compared to measured data for a subject not exhibiting CIVD response to cold stress. Conformity of calculated and measured data was very good with a maximum deviation of less than 10% at only one point in time. Results of this

20 DISTRIBUTION/AVAILABILITY OF ABSTRACT ☒ UNCLASSIFIED/UNLIMITED ☐ SAME AS RPT ☐ DTIC USERS	21 ABSTRACT SECURITY CLASSIFICATION UNCLASSIFIED
22a NAME OF RESPONSIBLE INDIVIDUAL Avraham Shitzer, Ph. D.	22b TELEPHONE (Include Area Code) 508/651-5140	22c OFFICE SYMBOL SGRD-UE-ME

DD Form 1473, JUN 86   Previous editions are obsolete   SECURITY CLASSIFICATION OF THIS PAGE

19. ABSTRACT (cont'd)

study facilitate the estimation of lower bounds to thermally
insulated fingers and toes exposed to cold stress.

CONTENTS

LIST OF FIGURES

LIST OF TABLES

ACKNOWLEDGEMENTS

EXECUTIVE SUMMARY

Military operations in cold climates require that soldiers be maintained relatively warm for safety and optimum performance. Protection afforded by passive cold weather clothing ensembles may be limited in duration. This problem is accentuated under inactive conditions and, particularly, in relation to the extremities and the exposed parts of the face. These body elements, even when protected by thermal insulation, e.g., gloves, may cool down to temperature levels which may endanger the soldiers' safety and ability to operate. Knowledge of endurance times associated with these exposures, is, therefore, of prime importance to the military commander. In this study, the estimation of endurance times, as it pertains to the digits, is performed by a one-dimensional, cylindrical model depicting these body elements. An analytical solution of the axial temperature variations is obtained in terms of an infinite series. Thermal and physical properties specified for the model pertain to the modeled body parts and to typical insulation layers applied. Blood perfusion effects are lumped into a volumetric heat generation term. Cold-induced vasodilatation (CIVD) effects were not included in the present analysis. Endurance times, as determined by a drop of cylinder (digit) tip temperature to 5^0 C were evaluated. Parameters included in this evaluation were: (a) environmental temperatures, (b) thermal insulation applied on the cylinder, (c) length of the cylinder, and, (d) diameter of the cylinder. It was found that the lower the temperature, the longer the finger, and the smaller the diameter thereof - the shorter is the endurance time for the same thermal insulation. Results of the model were compared to measured data for a subject not exhibiting CIVD response to cold stress. Conformity of calculated and measured data was very good with a maximum deviation of less than 10% at only one particular point in time. This model facilitates the conservative estimation of lower bounds to thermally insulated fingers and toes exposed to cold stress.

INTRODUCTION

Humans are often required to occupy and operate in cold climates. The limited natural ability to cope with extreme environmental conditions must be supplemented by auxiliary means if humans are to survive and function effectively under harsh conditions. One of the common means employed to cope with cold environments, is the use of clothing to increase thermal insulation. In many cases the protection afforded by clothing is sufficient but there may be situations wherein certain body parts, most notably the extremities and the face, are still not adequately protected. This may occur particularly under prolonged sedentary conditions in very cold environments [1]. This report analyzes the temperature changes of the extremities, particularly fingers (digits) and toes during cold stress.

The reasons for the susceptibility of these body elements to cold temperatures are both physiological and physical in nature. The physiological reason relates to the main heat source in an extremity, e.g., finger, which is its blood supply. Under neutral environmental conditions, the flow of blood and the associated internal generation of metabolic heat are usually sufficient to maintain finger temperatures within a safe and comfortable range. Upon exposure to cold temperatures, however, blood flow to the fingers is constricted, primarily as a means for conserving heat. This causes a significant diminution of the supply of heat to the finger. Values in the literature indicate a drop in blood perfusion rate from about 15-40 to only about 1 cc/(min 100 cc) [2 cited in 3]. An even higher range of variability, of about 100 fold, was also suggested [1].

One of the physical reasons for the susceptibility of fingers to cold environments is due to their shapes, which resemble slender cylinders. These cylinders act like heat transfer fins. The result is enhanced heat loss to the environment, with an ensuing accelerated drop in finger temperature. This physical property of an extremity is not specific to cold exposures. Its effects, however, are much more pronounced under such conditions, mainly due to the increased temperature difference.

An additional physical limitation relates to the thickness of thermal insulation which may be applied on cylindrical surfaces. Since the surface of a cylinder is curved, each layer of applied insulation would be of a larger diameter and hence of an increased surface area. Thus, there is a "critical" thickness beyond which heat loss to the environment would be increased, rather than decreased. This limitation does not apply to insulation applied to flat

2

surfaces due to the absence of curvature. In the context of this study, gloves may be considered to provide individual layers of insulation to each finger. Mittens are different in that they usually cover all four fingers at once, except the thumb. They can, therefore, be made thicker, or more insulative, compared to the size limitations imposed on the finger covers in gloves.

Van Dilla et al. [3] have estimated the insulation required to maintain finger temperatures at comfortable levels of $15.5^\circ C$ ($60^\circ F$) or $28.9^\circ C$ ($84^\circ F$) under different internal heat generation rates and environmental temperatures down to $-40^\circ C$ ($-40^\circ F$). They performed a steady state analysis and simulated the application of fabrics to either cylinders, spheres or plane surfaces, depicting, finger shaft, fingertip and hand, respectively. Assuming that "one quarter of an inch of fabric thickness may be taken as the maximum thickness consistent with reasonable dexterity", the authors concluded that the finger could be protected by a maximum insulation value of about 0.9 clo [3]. This finding demonstrates the limitations imposed by physical laws, on the one hand, and the physiological response of vasoconstriction, on the other. Van Dilla et al. further extended their analysis to mittens concluding that "mittens are decidedly superior to gloves in both insulation value and efficiency of fabric utilization". This conclusion holds, however, at the expense of rendering the mittens "highly cumbersome, unwieldy and impractical".

Using Hatch's equation of body cooling, Van Dilla et al. estimated the tolerance times for the average finger skin temperature to drop to $8.9^\circ C$ ($48^\circ F$) from an initial temperature of $33^\circ C$ ($91.4^\circ F$), while covered by a certain mitten. They found that at $-40^\circ C$ ambient temperature, the tolerance times, for different heat generation rates, were 80-85 min compared to experimentally determined 75 min. At $-23.3^\circ C$ ($-10^\circ F$) and $-6.7^\circ C$ ($20^\circ F$) the calculated tolerance times were 156-184 min and 132 min, respectively. These calculated times compared favorably with those determined experimentally, 180 min and 137 min., respectively, for these two conditions.

Molnar analyzed the rate of digital cooling to the freezing point [4]. He assumed Newton's law of cooling to apply and a uniform temperature throughout the digit. Fingers were exposed, without insulation in a small "wind tunnel", to a $-15^\circ C$ environment with wind at 10 m/sec. Finger temperatures were observed to fall to $-6.2^\circ C$, or even lower, before freezing occurred followed by a quick rewarming to about $-2.4^\circ C$ due to the "evolution of (latent) heat". In certain experiments, conducted under similar conditions, no freezing was observed to have occurred, indicating the onset of cold induced vasodilatation (CIVD).

3

Molnar concluded his study by stating that "there was no correlation between the elapsed time to the onset of freezing and the relative cooling rate". He also suggested the possibility that CIVD started when a particular skin temperature was reached but refrained from giving any further details.

Wilson and Goldman [5] and Wilson et al. [6] studied the freezing temperatures of finger skin. Their results indicate that in the majority of cases, 50 out of a total of 72, skin freezing did occur under the conditions of the study. The mean supercooled skin temperature at which frostnip appeared was -9.4°C followed by an average temperature rise of 5.3°C due to the absorption of the heat of fusion at ice crystallization [6]. Wilson and Goldman suggest that below a wind chill of 1400 and for air temperatures in the range of -10° to -15°C, freezing of fingers rarely occurs [5].

Goldman discussed the problem of protecting the inactive Arctic soldier for 8 hours in a -40°C environment with a 1.34 m/sec (3 mph) wind [1]. As a consequence of vasoconstriction, the hands and feet become the limiting factors in tolerance to cold. He showed that, under these conditions no passive protection was possible and that auxiliary heating was required. Results show that electrical resistance heating of gloves and socks may be the most practical means of maintaining the extremities at any desired temperature level between 10°C (50°F) and 40.2°C (105°F). The minimal power requirements, for maintaining the extremities above 4.4°C (40°F), were 3 W and 7 W for the hand and foot, respectively. Goldman found that the mean times to cool from maintained 5th finger temperatures of 26.7°C (80°F) or 15.6°C (60°F) to 4.4°C (40°F), after power was shut off to the heated glove, were 6.7 and 4.1 min, respectively. When a windproof leather glove shell was provided over the heated glove, these times became slightly longer at 9.6 and 5.9 min, respectively.

An alternative to auxiliary heating of the hands and feet in cold environment is metabolic heat generated by physical activity. This, however, may not always be totally effective, depending on the environmental conditions and level of activity. Santee and co-workers [7], studied the effects of cold weather handwear used by petroleum handlers who were required to operate manual pumps intermittently. Their experiments were conducted in a -34.4°C (-30°F) and a 2.2 m/s (5 mph) wind speed environment. Initial results indicated that endurance times, determined when a finger temperature reached 5°C, barely exceeded 10 min. When both pre-test conditions were adjusted and test chamber temperature was raised to -28.9°C (-20°F), endurance times, including pumping times, increased considerably to

between about 27 and 33 minutes. The authors showed that middle finger nail bed temperature varied appreciably in subjects demonstrating the fast initial drop followed by oscillations due to the alternating pump-rest cycles.

The purpose of the present report is to analyze the factors affecting the thermal response of a finger-like, cylindrical model. A one-dimensional analytical model of the axial temperature variations of this model is formulated. The model is solved by an orthogonal transformation and is presented in terms of an infinite series. The effects of finger insulation, length and diameter and those of the environmental temperature, were studied. Analytical predictions of the model were compared to experimental data and a very good conformity was obtained.

ANALYSIS

Consider the right angle circular cylinder, shown in Fig. 1, to depict any body element which may be approximated by this geometry, e.g., fingers, toes, arms, etc. This cylinder is exchanging energy with the environment through its exposed surfaces. Inside the cylinder heat flows from one location to another only by conduction. In addition, there is heat exchange at the base of the cylinder due to its attachment to the proximal body element, e.g., hand in the case of a finger.

For simplicity, the following assumptions are made:
(a) The thermophysical properties of the cylinder are uniform and isotropic.
(b) Metabolic heat is generated at a uniform rate in the cylinder, which may vary in time.
(c) Due to the aspect ratio of the cylinder, radial heat conduction is ignored as compared to axial conduction.
(d) Blood perfusion effects on heat exchange are not included directly in the model, but are lumped into the term describing metabolic heat generation.

Conservation of energy requires that the following balance be maintained in each infinitesimal element of the cylinder:

$$\begin{Bmatrix} CHANGE\ IN \\ STORED \\ ENERGY \end{Bmatrix} = \begin{Bmatrix} ENERGY \\ CONDUCTED \\ INTO \end{Bmatrix} - \begin{Bmatrix} ENERGY \\ CONDUCTED \\ OUT\ OF \end{Bmatrix} + \begin{Bmatrix} ENERGY \\ GENERATED \\ INSIDE \end{Bmatrix} - \begin{Bmatrix} ENERGY\ LOST \\ TO\ THE \\ ENVIRONMENT \end{Bmatrix}$$

5
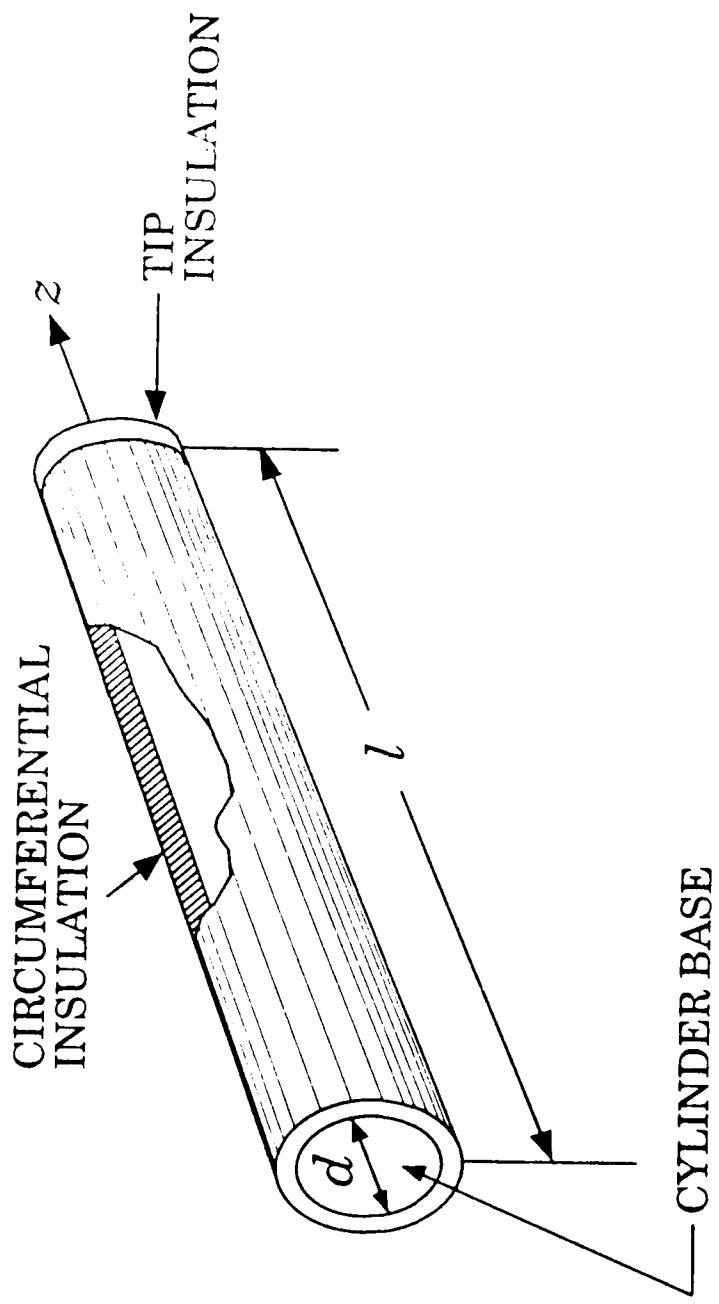
Figure 1. Schematic diagram of the cylindrical model showing the thermal insulation applied.

In mathematical notations this heat balance may be written as:

$$\rho c \frac{\partial T}{\partial t} = k \frac{\partial^2 T}{\partial z^2} + q - \frac{ph}{A}(T - T_o) \tag{1}$$

where: ρ is density, c is specific heat, T is temperature, t is time, k is thermal conductivity , z is axial coordinate, q is metabolic heat generation rate per unit volume, p and A are cylinder circumference and cross-section area, respectively, h is heat transfer coefficient between the cylindrical surface and the environment and T_o is environmental temperature.

Equation (1) is solved subject to the following boundary and initial conditions:
At the base of the cylinder a variable temperature is assumed

$$T = T_1(t) \qquad @ \ z = 0, \ t \geq 0 \tag{2}$$

At the tip of the cylinder, convective heat exchange with the environment occurs:

$$-k \frac{\partial T}{\partial z} = h_1(T - T_0) \qquad @ \ z = \ell, \ t \geq 0 \tag{3}$$

where h_1 is the heat transfer coefficient between the tip of the cylinder and the environment which may be different than that assumed for the circumferential area of the cylinder, h.

The initial condition for the axial temperature in the cylinder is given by an arbitrarily specified distribution

$$T = T_i(z) \qquad @ \ t = 0, \ 0 \leq z \leq \ell \tag{4}$$

The solution to the above set of equations is obtained by employing an orthogonal integral transformation [8] and [9]. Steps performed in the derivation of the solution are discussed in Appendix A. The result obtained is

$$T(z,t) = \ell \sum_{n=1}^{\infty} \{ \tau - \alpha \int_0^t G(\eta) \exp(\alpha \lambda^2 \eta) d\eta \} \exp(-\alpha \lambda^2 t) \sin\frac{\beta_n z}{\ell}$$
$$+ T_0 - f_1(z)[T_1(t) - T_0] \tag{5}$$

where,

$$\tau = B_n \int_0^\ell [T_i(z) - T_o] \sin\frac{\beta_n z}{\ell} dz - \frac{B_n \ell}{\beta_n} F_o(o) \tag{6}$$

$$B_n = \frac{2(\beta_n{}^2 + Bi^2)}{\ell^2(\beta_n{}^2 + Bi^2 + Bi)} \tag{7}$$

$$G(t) = \frac{B_n \ell}{\beta_n}\{LF_0(t) + \frac{1}{\alpha}\frac{dF_0}{dt}\} + \frac{q(t)\ell B_n}{k\beta_n}(\cos\beta_n - 1) \tag{8}$$

$$F_0(t) = T_1(t) - T_o \tag{9}$$

$$f_1(z) = \frac{Bi}{1+Bi}(\frac{z}{\ell}) - 1 \tag{10}$$

and,

$$\beta_n \cot\beta_n = -Bi \tag{11}$$

The general solution, Eq. (5), contains a number of operations to be carried out. These

8

operations are either integrals in Eqs. (5) and (6), or the solution of a transcendental eigenvalue equation (10). Performance of all indicated operations depends on the specific value of B_i in Eq. (10), the specific initial condition $T_i(z)$, Eq. (6), and the values specified for both the time dependent boundary condition at the base of the cylinder, $T_1(t)$, and the metabolic rate, $q(t)$, in Eq. (8). These operations would now be carried out for a set of selected values and functions. Obviously, different values and functions may be selected and substituted into the appropriate expressions.

Solution of the eigenvalue equation (10), may be obtained by a number of well-established techniques. Two parameters will have to be specified: B_i and the acceptable cut-off accuracy to be employed by the solution algorithm. In the present case, a combination of solution techniques was chosen, each one is applied for a different range of the parameter B_i. For low and negative values of $B_i < 1.37$, a Newton-Raphson procedure is employed. For $B_i > 1.37$, a parameter-adjusted axis-crossing routine is applied. In all cases, care is taken to insure that all successive eigenvalues are calculated and the cut-off accuracy chosen is usually of the order of 10^{-4}, particularly for the first ten eigenvalues. The calculation procedure, employing double-precision, was programmed in Turbo-Pascal and is included in the listings presented in Appendix B. A sample output of results is given in Table 1.

Next, the integration indicated in Eq. (6), is carried out for a specific example:

$$
\begin{aligned}
\tau &= B_n \int_0^{\ell} [T_i(z) - T_o] \sin\frac{\beta_n z}{\ell} dz - \frac{B_n \ell}{\beta_n}(T_1(0) - T_0) \\
&= \frac{B_n \ell}{\beta_n} \int_0^{\beta} T_i(z) \sin\zeta \, d\zeta + T_o \cos\beta_n - T_1(o)
\end{aligned}
\tag{12}
$$

It is assumed that the initial temperature distribution in the cylinder is linear:

$$
T_i(z) = (T_3 - T_2)\frac{z}{\ell} + T_2
\tag{13}
$$

which yields, upon substitution and integration:

$$\tau = \frac{B_n \ell}{\beta_n} \{ \frac{T_3 - T_2}{\beta_n} \sin \beta_n + T_2 - T_1 - (T_3 - T_o) \cos \beta_n \} \tag{14}$$

Equation (14) holds also for the specific case of an initially uniform temperature by assigning $T_2 = T_3$. Other forms, including piecewise initial temperature distributions, may be accommodated.

Finally, time-dependent, exponentially-decaying functions are assumed for the cylinder base temperature $T_1(t)$ and the metabolic heat generation rate $q(t)$, respectively:

$$T_1(t) = T_f + (T_i - T_f) \exp(-t/\delta) \tag{15}$$

$$q(t) = q_f + (q_i - q_f) \exp(-t/\varepsilon) \tag{16}$$

where subscripts f and i indicate final and initial values, respectively, and δ and ε are the time constants for the base temperature and metabolic heat generation rate, respectively.

In summary, and for the specific functions [Eqs. (13), (15) and (16)] chosen here, the temperature of the cylinder is given by

$$T(z,t) = T_o + \ell \sum_{n=1}^{\infty} \{ [\lambda_n^2 \tau + C_n + G_n + H_n] \exp(-\alpha \lambda_n^2 t) $$

$$- C_n - G_n \exp(-t/\delta) - H_n \exp(-t/\varepsilon)) \frac{\sin \beta_n \frac{z}{\ell}}{\lambda_n^2} \tag{17}$$

$$- [\frac{Bi}{1 + Bi} \frac{z}{\ell} - 1] \{ T_f + (T_i - T_f) \exp(-t/\delta) - T_o \}$$

10

TABLE 1: Sample array of the first 40 eigenvalues for Bi=0.6

INDEX	EIGENVALUE, β_n	RESIDUAL OF: $\beta_n \cot(\beta_n)$-Bi
1	1.868875893336337	-1.82260505531735566E-0005
2	4.830676037164286	7.62215668461966775E-0005
3	7.926291752979685	1.05305134443524871E-0005
4	11.047499501381431	2.79093696162852848E-0006
5	14.177642504858346	1.02861745192203398E-0006
6	17.311913171169223	4.62309653183909462E-0007
7	20.448423440435814	2.37149491793284348E-0007
8	23.586283165340159	1.33650781398314024E-0007
9	26.725021611627494	-8.75384552623320253E-0005
10	29.864355859361979	-6.97336170789010436E-0005
11	33.004119522373991	-5.66851208108707510E-0005
12	36.144200808375331	-4.68078387106063377E-0005
13	39.284523617986736	-3.91231265649041849E-0005
14	42.425034356955287	-3.30003129129237513E-0005
15	45.565694191642798	-2.80181546708159110E-0005
16	48.706474295923925	-2.38866133840582619E-0005
17	51.847352823254987	-2.04007117645318699E-0005
18	54.988312915192573	-1.74122659687615160E-0005
19	58.129341354865495	-1.48119995613488296E-0005
20	61.270427634230991	-1.25178993957863918E-0005
21	64.411563294015238	-1.04674449592920748E-0005
22	67.552741447665682	-8.61230079254881892E-0006
23	70.693956432130392	-6.91462260674405565E-0006
24	73.835203547724092	-5.34444082346335284E-0006
25	76.976478861650733	-3.87777149877312774E-0006
26	80.117779057723041	-2.49523848554927038E-0006
27	83.259101320085364	-1.18104864801584679E-0006
28	86.400443242290720	7.77715485750490182E-0008
29	89.541802755508613	1.29196504065475382E-0006
30	92.683178071327191	2.47047923332914922E-0006
31	95.824567635801671	3.62082767459327324E-0006
32	98.965970092251780	4.74934312700713186E-0006
33	102.107384250924127	5.86140509312643243E-0006
34	105.248809064086231	6.96159955776171763E-0006
35	108.390243605450252	8.05385984536152299E-0006
36	111.531687053073284	9.14156880406797332E-0006
37	114.673138675067463	1.02276585760379107E-0005
38	117.814597817595924	1.13146708342631462E-0005
39	120.956063894738790	1.24048257638330025E-0005
40	124.089269053266150	1.02594436089180108E+0000

where,

$$C_n = \frac{B_n \ell}{\beta_n} \{ L(T_f - T_o) + \frac{q_f}{k} (\cos \beta_n - 1) \} \tag{18}$$

$$G_n = \frac{B_n \ell}{\beta_n} \frac{\lambda_n^2 (T_l - T_f)(\alpha \delta L - 1)}{\alpha \lambda_n^2 \delta - 1} \tag{19}$$

$$H_n = \frac{\alpha \ell B_n}{k \beta_n} (\cos \beta_n - 1) \frac{\lambda_n^2 \varepsilon (q_l - q_f)}{\alpha \lambda_n^2 \varepsilon - 1} \tag{20}$$

and τ, λ_n^2, β_n, Bi and B_n are defined by Eqs. (12), (A.32), (11), (A.16) and (7), respectively.

Equation (17) was programmed in Turbo Pascal and a listing is given in Appendix B.

RESULTS AND DISCUSSION

The present model may be studied by selecting a set of parameters and evaluating its behavior. The parameters should be selected to depict, as closely as possible, realistic values pertaining to the modeled entity. In the present case these parameters should represent biological tissues and their thermophysical as well as anthropometric properties. In addition, there are external conditions to be specified, e.g., environmental temperature, insulation applied, model initial condition, etc.

The number of possible combinations of parameters is almost infinite. The advantage afforded by an analytical model is in its ability to facilitate the study of specific parameters at a relatively low cost and without the need for elaborate and costly experiments. However, the ultimate test of a model is in its ability to closely predict the behavior of the modeled

12

entity. This may be tested by comparing model predictions to experimental results.

In the present study, three cases were studied and are presented below. All cases were assumed to relate to the behavior of fingers, i.e., digits, covered by gloves of different insulating values. Parameters employed in the calculations are listed in Table 2.

In the first case, a constant digit base temperature and metabolic heat generation rate are assumed. Results are shown in Figs. 2 and 3, for an environmental temperature of -5°C. Digit base temperature is maintained at 30°C throughout the exposure and a total heat transfer coefficient of 7.12 W/m² °C representing an insulation value of about 0.9 clo. The initial temperature in the digit is assumed to be linear from 30°C to 20°C, as shown in Fig. 2. The other curves in this figure show the temporal evolution of the axial temperature distributions along the digit until a final steady state is reached. As is to be expected, digit temperatures decrease monotonically until finally a large temperature gradient, of about 30°C in this case, has been established between the base and the tip of the digit.

TABLE 2: Typical parameters used in the calculations
(parentheses indicate default values)

|	
Thermal conductivity, $W\ m^{-1}\ C^{-1}$	0.418
Thermal diffusivity, $m^2\ hr^{-1}$	0.0004546
Heat transfer coefficient, $W\ m^{-2}\ C^{-1}$	5 - 12
Digit length, m	0.06 - 0.12 (0.08)
Digit diameter, m	0.01 - 0.0175 (0.015)
Metabolic heat generation rate, $W\ m^{-3}$	
initial, or constant	15000 - 29000 (15000)
final	15000 - 26500 (15000)
Environmental temperature, C	0 to -20
Initial digit temperature (linear), C	30 to 20
Exponential time constants, hr	
metabolism	0.4
digit base temperature	1.3
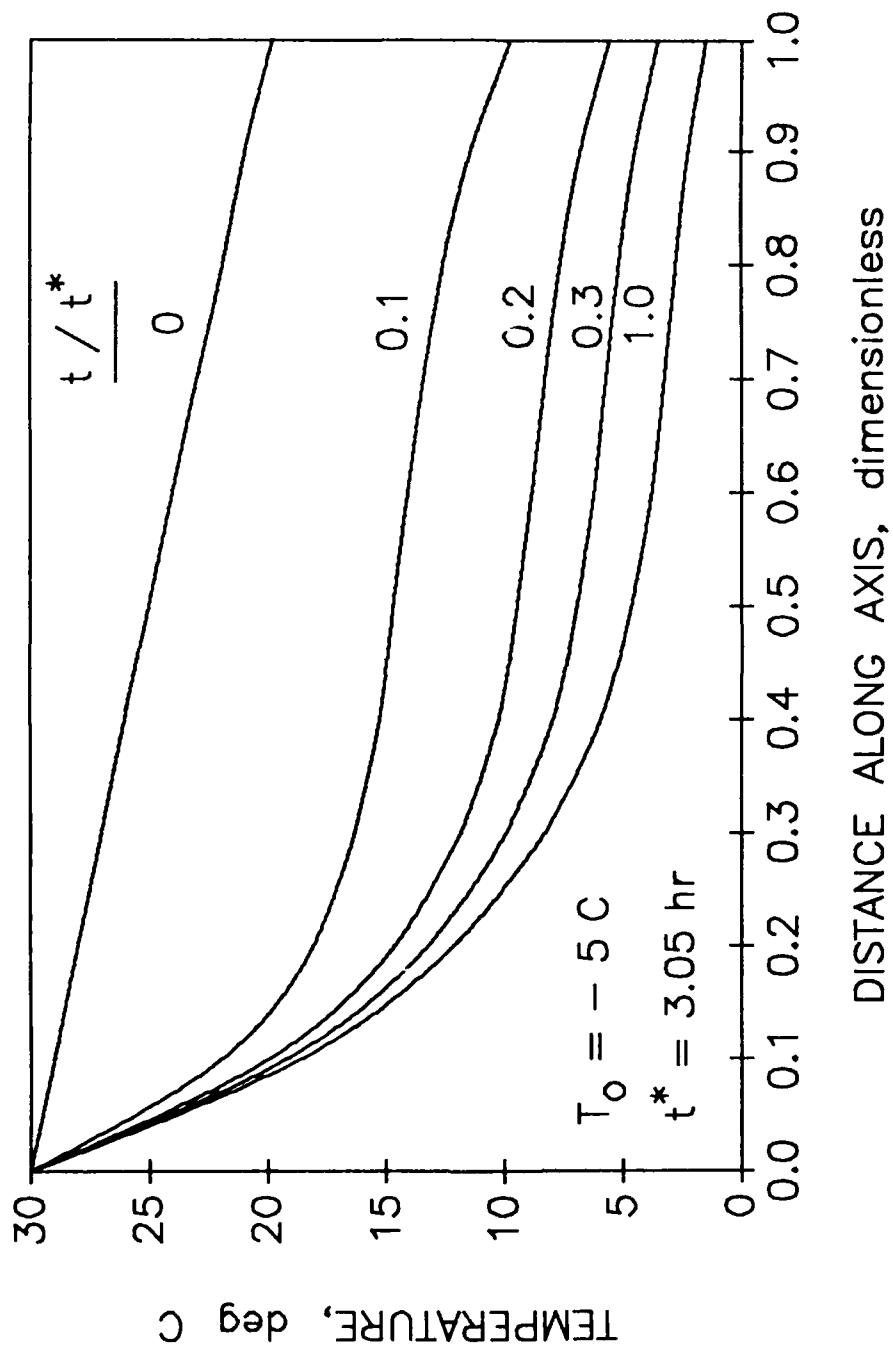
Figure 2. Temperature distribution along digit axis for constant base temperature and metabolic heat generation rate.

Figure 3 shows temperature variations at different locations along the digit. The uppermost curve is plotted for Z=0, or digit base, whereas the lowest curve indicates digit tip. The total time for which both Figs. 2 and 3 were calculated is about 3.05 hrs. At this time a final steady state has been established throughout the entire digit. However, inspection of Fig. 3 reveals that, for all intended purposes, a practical steady state becomes established much sooner, at about 1 hour and 30 minutes. This is also indicated in Fig. 2 by the convergence of the curves at the final temperature. Thus, the curve indicating the final temperature distribution in the digit at 3.05 hrs is quite close to that calculated for less than an hour ($t/t^*=0.3$) from the beginning of the exposure.

One of the more practical results that may be deduced from Fig. 3 relates to the time it would take to reach a certain temperature anywhere in the digit. Of particular interest is the tip of the digit, which undergoes the most extreme temperature changes. Suppose 5°C is selected as a limiting digit tip temperature, according to accepted experimental procedures involving cold exposures [10]. Under the conditions selected for Fig. 3, it would take about 44 minutes for the tip temperature to drop to 5°C. Another useful application of the model could be the prediction of exposure times for onset of frostbite or frostnip. Under the present set of parameters, Fig. 3 indicates that the minimal temperature at the digit tip would remain above 0°C, indicating no imminent danger of freezing.

Figures 4 and 5 are plotted for a case similar to the previous one except that both digit base temperature and rate of metabolic heat generation are assumed to vary exponentially according to Eqs. (15) and (16), respectively. One consequence of this difference is in a slightly larger time to reach steady state, 3.28 hrs compared to 3.05 hrs. The reason for this prolonged time is due to the lower final temperatures obtained in this case, Figs. 2 vs. 4. Thus, more heat must be extracted and the digit takes longer to reach a steady state.

Tip temperatures of the left little finger measured in this laboratory at the nail bed under sedentary conditions [11], are compared to model predictions. The comparison is given for two different environmental temperatures: -6.7°C in Fig. 6 and 0°C in Fig. 7. Of all experimental conditions and subjects employed in this study [11], the particular case selected for comparison is the one not involving any activity and for the subject exhibiting minimal cold-induced vasodilatation (CIVD) response. This was done since the present model does not incorporate this phenomenon. It should be pointed out, however, that the lack of a CIVD response to cold exposure of the fingers may be present among a portion of the population. This makes such individuals, particularly those suffering from Raynaud's phenomenon, more
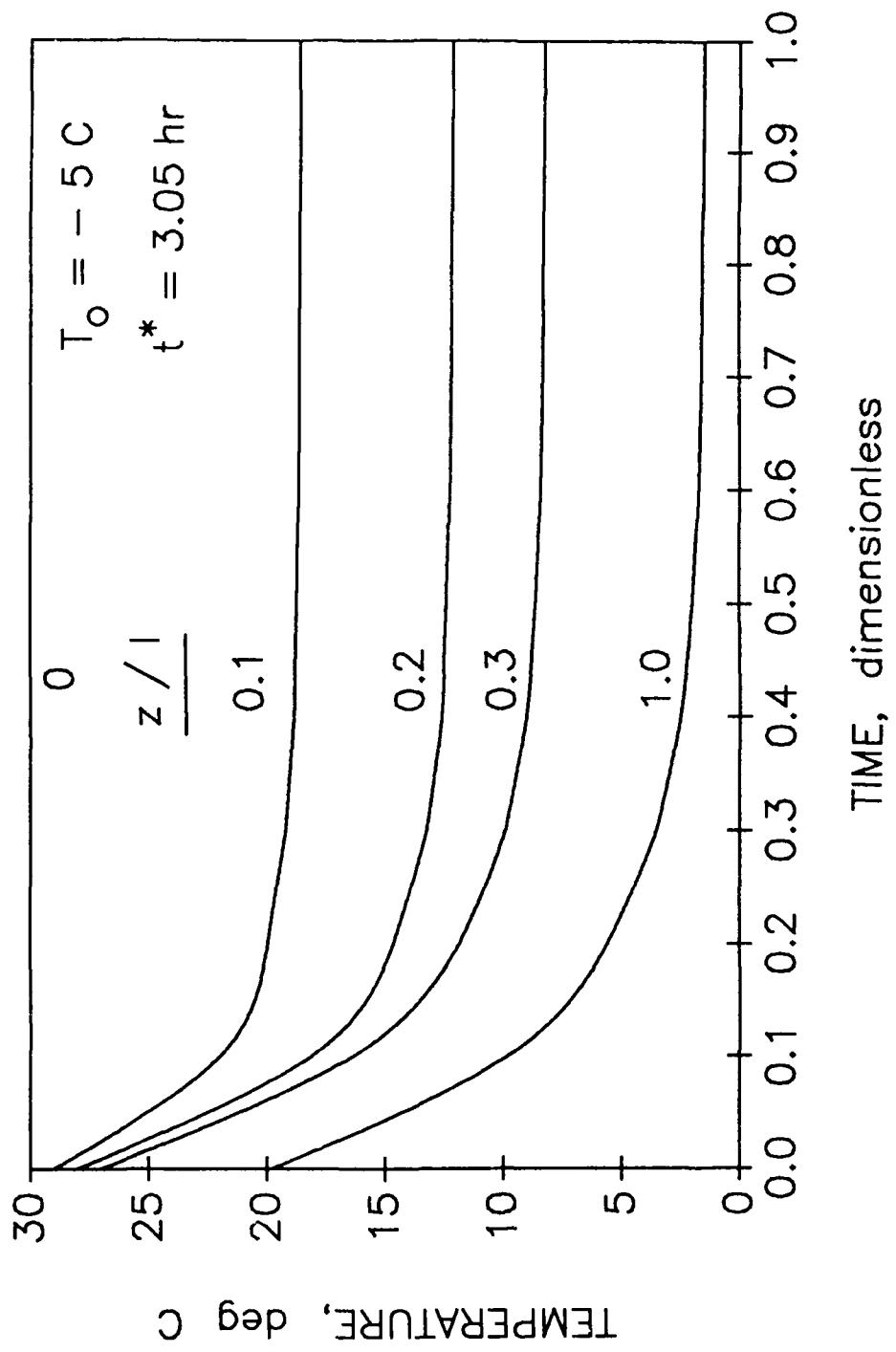
Figure 3. Temperature variations at different points in the digit for constant base temperature and metabolic heat generation rate.
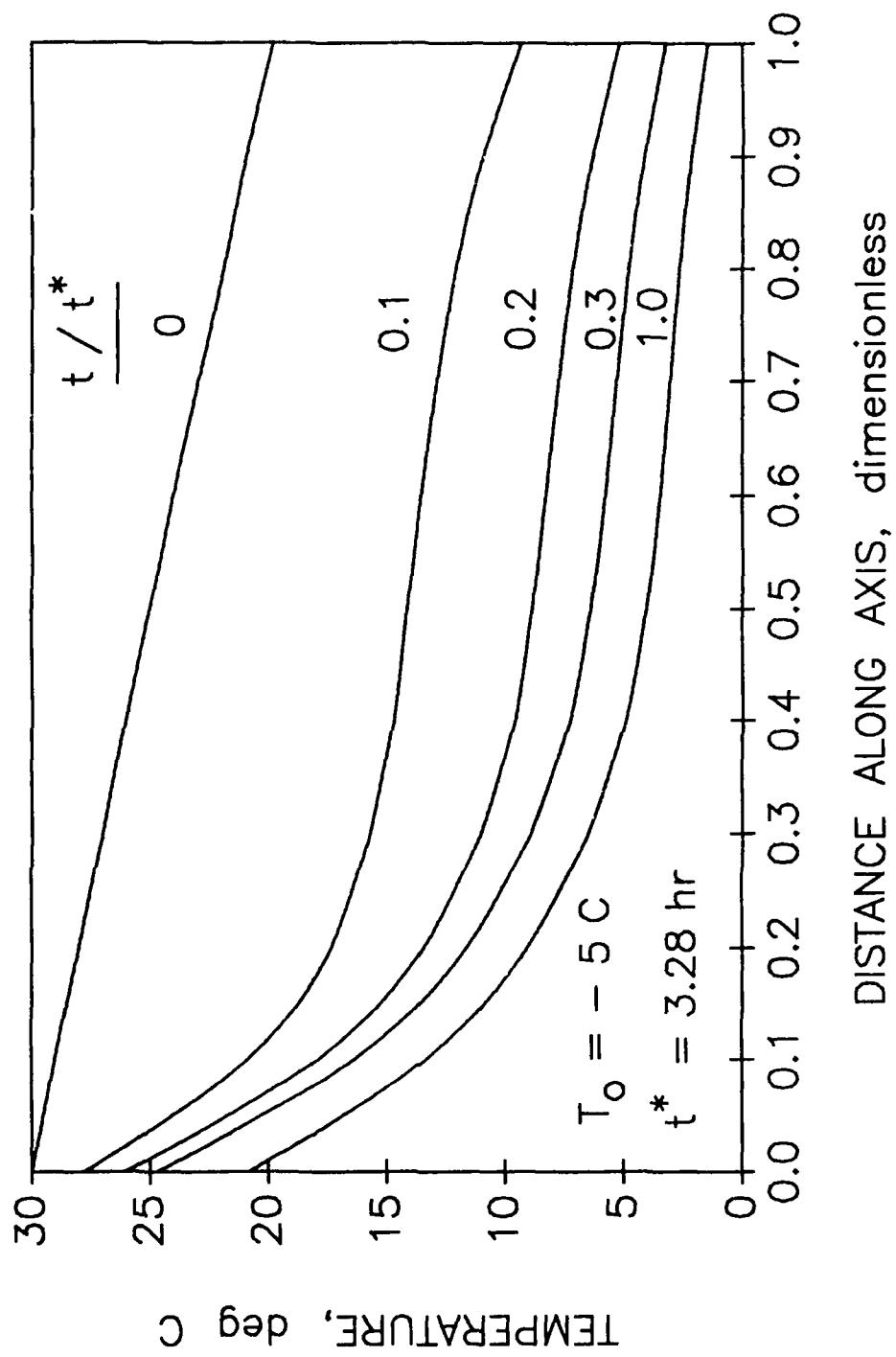
Figure 4. Temperature distributions along digit axis for variable base temperature and metabolic heat generation rate.
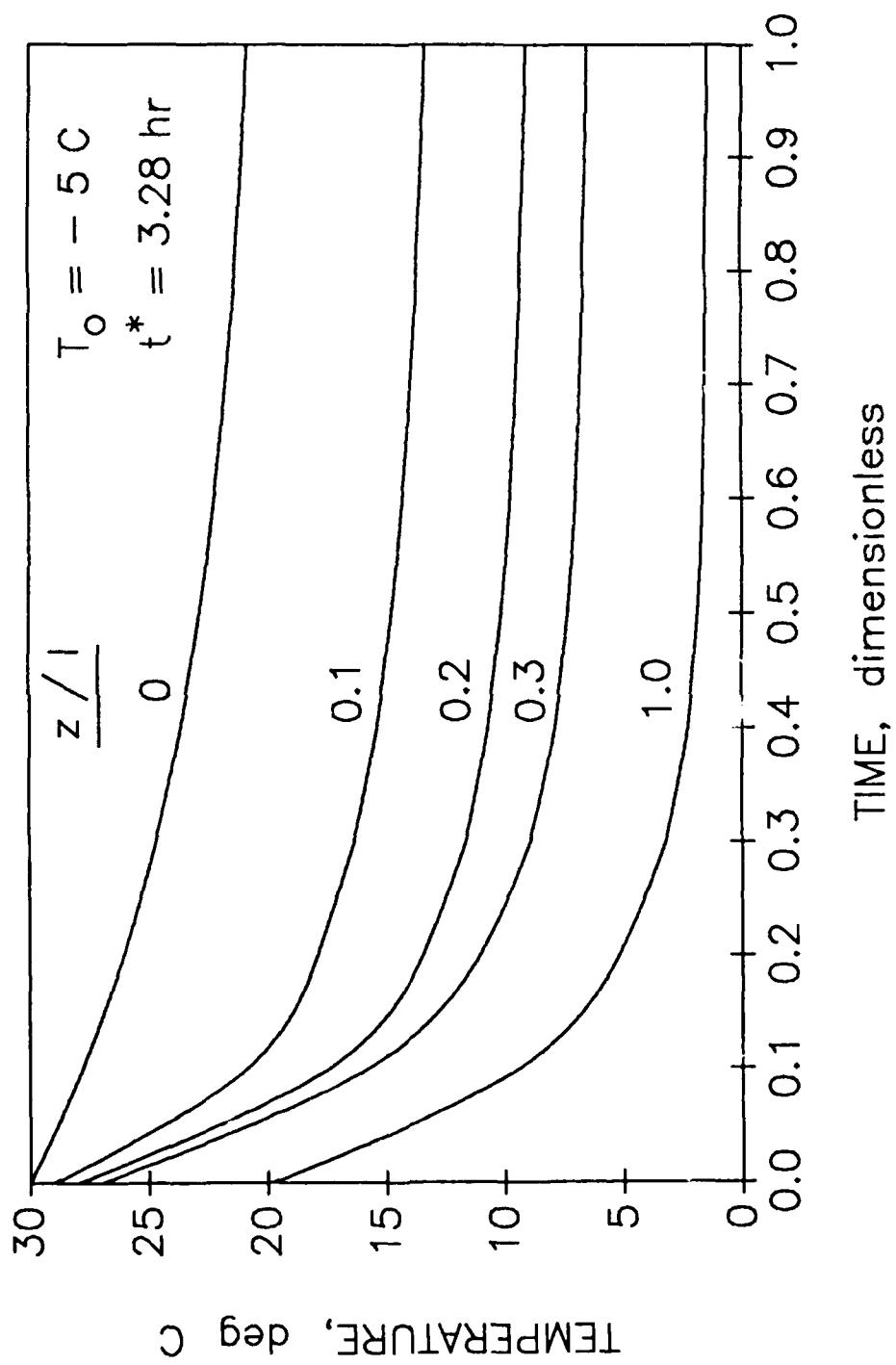
Figure 5.   Temperature variations at different points in the digit for variable base temperature and metabolic heat generation rate.

vulnerable to the effects of cold stress [12]. The lack of CIVD response is not, however, limited to people suffering from this disease.

Parameters selected for calculating model predictions were based, as much as was possible, on actual values reported in the study and on established thermophysical properties. Thus, a 0.9 clo (converting to $h=h_1=7.12$ W $m^{-2}{}^{\circ}C^{-1}$) was used for the thermal insulation applied on the finger and finger tip. Finger length was set at 6.5 cm and finger diameter at 1.78 cm. Initial finger base temperature was set at 33°C and was allowed to drop to a final value of 20°C with an exponential time constant of 1.3 hrs, Eq. (16).

The only parameter not accounted for in the data available was the rate of metabolic heat generation. In the present study this property accounts for the combined effects of both the intrinsic rate of metabolic heat generation and the amount of heat transported by blood circulation. Of these two mechanisms the latter is by far the dominant one and may reach high values, depending on the flow rate and temperature difference. Thus, the total combined rate of heat generation, $\dot{q}$, was estimated using minimal blood perfusion rates of 0.5 - 1.5 cc/(100 cc·min) [1,2] and a temperature difference of about 20-25°C. Based on these assumptions, and the conformity of calculated to measured data, the $\dot{q}$ used in Fig. 6 was 29,000 W/m³, decaying exponentially to 27,500 W/m³ with a time constant of 0.4 hours. For Fig. 7, the value used was smaller, 16,500 W/m³, which was maintained constant.

Both Figs. 6 and 7 show quite good conformity of calculated vs. measured data. The largest deviation, of the order of about 1.5°C, occurs after about 30 minutes in Fig. 6, indicating fluctuations in blood flow. In both Figs. 6 and 7 there are indications of weak vasomotor activities toward the end of the experiment. This phenomenon is particularly pronounced in Fig. 7 which otherwise shows few fluctuations in finger tip temperature.

The duration of the two experiments was different, 85 and 105 minutes in Figs. 6 and 7, respectively. In both experiments, finger tip temperature dropped to about 9°C at the end of the exposure. The model facilitates the estimation of the final finger tip temperatures and the times to reach these levels. Calculations show that, in both cases, the final steady state temperatures would remain at the safe level above 5°C. Accordingly, the finger tip temperatures would reach about 7°C and 8.4°C after about 280 and 237 minutes, respectively, for the -6.7°C and the 0°C environments.

To further investigate endurance times, defined here as the time for finger tip to reach

19
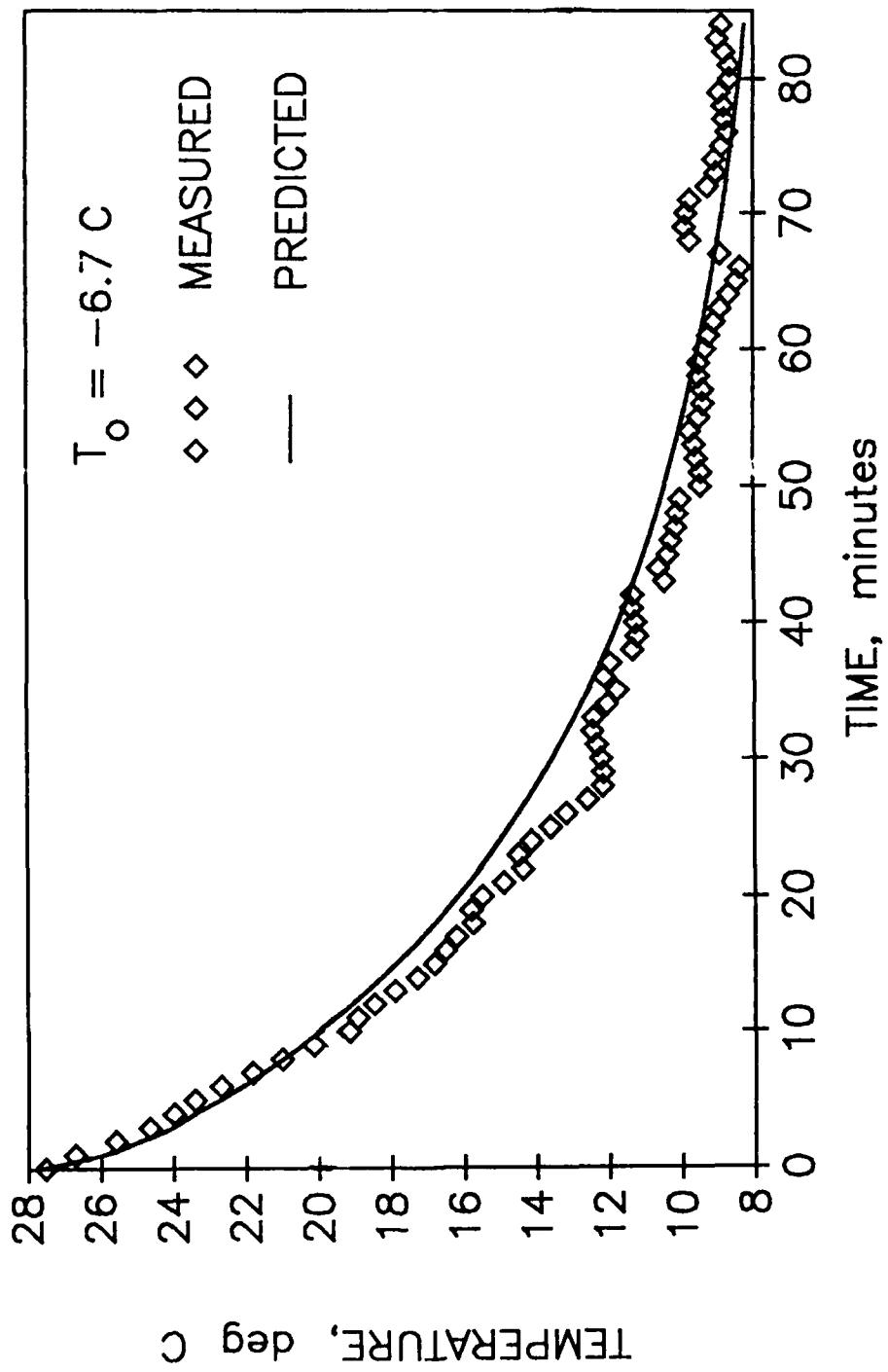
Figure 6. Comparison of measured vs. calculated temperature variations at left little finger tip of subject #5 at -6.7°C environment.
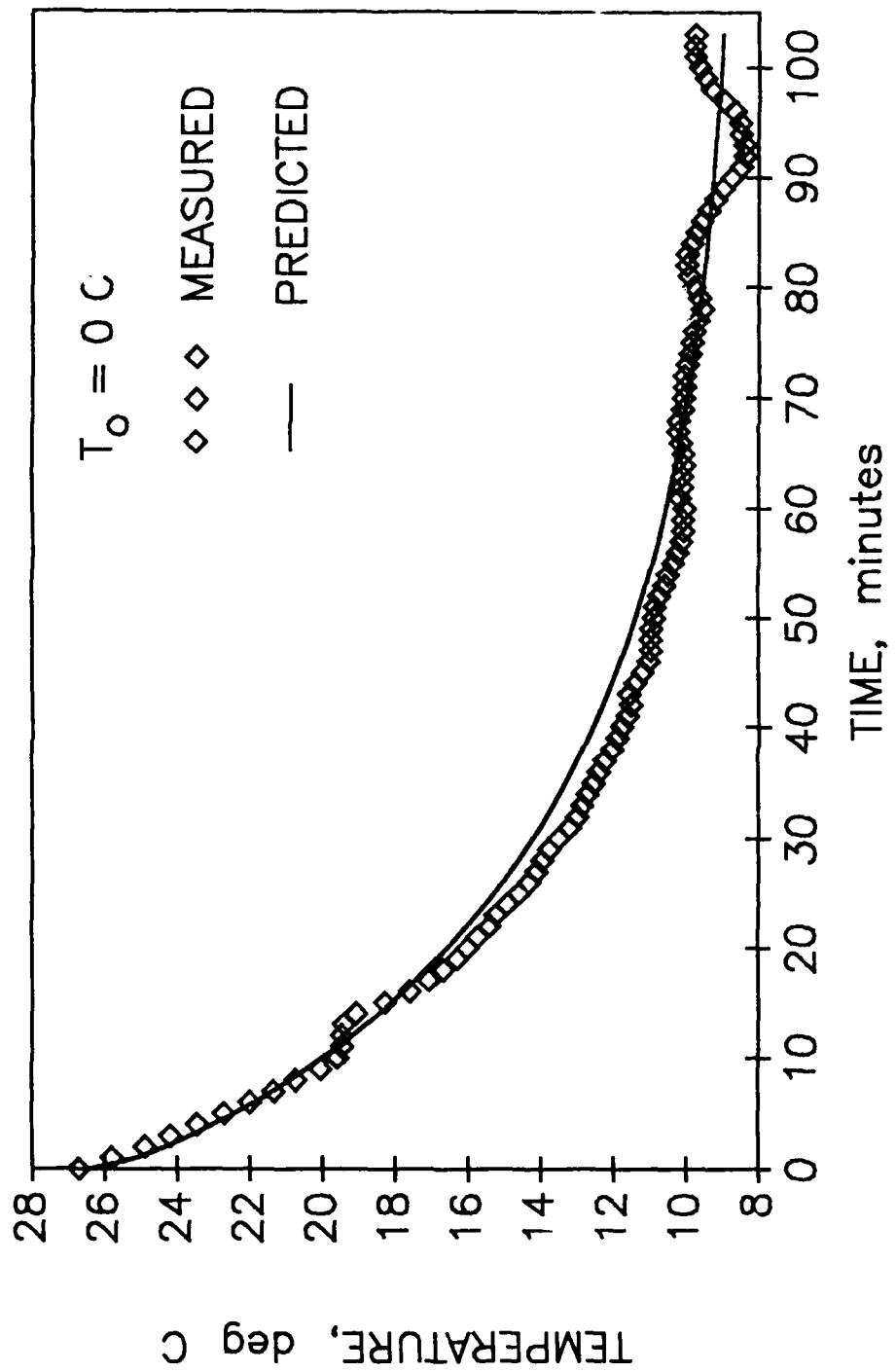
Figure 7.   Comparison of measured vs. calculated temperature variations at left little
finger tip of subject #5 at 0°C environment.

21

5°C, a parametric analysis was performed. Four parameters were chosen for this analysis: heat transfer coefficient of the insulation applied to the digit, environmental temperature, digit length and digit diameter. Results of these analyses are shown in Figs. 8-10.In all cases a 5°C digit tip temperature was chosen to designate a limiting temperature for which an endurance time may be calculated. In all cases presented here, digit base temperature and metabolic heat generation rate varied exponentially.

Figures 8-10 indicate the trends for endurance times quite clearly. Accordingly, the lower the environmental temperature (Fig. 8), the longer the digit is (Fig. 9), the smaller the digit diameter is (Fig. 10), the shorter the endurance times. An interesting result in Fig. 9 points out the fact that beyond a certain value of the heat transfer coefficient, endurance times are no longer sensitive to digit length. In the present case insulative values equal to about 0.9 clo (h=7.12 W/m^2 °C), or less, would entail essentially the same endurance times, regardless of digit length.

In order to evaluate the predicted endurance times, two values calculated by Santee et al. [11] are indicated by filled circles in Fig. 8. These values represent the average endurance times obtained for the sedentary experiments in a -6.7°C environment for two different gloves. It is seen that results of the model underpredict the measured values by a factor of about 2. This seemingly large disparity may easily be reconciled by recalling the fact that the values plotted in Fig. 8, were calculated for situations devoid of a CIVD response. The measured values, however, were obtained for a group of subjects, most of whom showed active CIVD behavior. Thus, they were able to allow periodic fluctuations in the blood supply to the fingers. This increased the availability of heat in the finger, considerably prolonging the endurance times over those indicated for the non-CIVD cases.

Indeed, when the total heating rate is increased from 15,000 W/m^3, used in Fig. 8, to about 29,000, used in Fig. 6, model results invert to overpredict the average measured values by about a factor of 2. It is to be expected, therefore, that the proper inclusion of the CIVD phenomenon, would make model predictions more realistic when applied to normal populations.

This discussion indicates the apparent limitations of the present model and the need for further development. The main usefulness of the present model is that it can provide a systematic database for assessing lower bounds for endurance times under quite a variety of physiological conditions as and physical parameters. These lower bounds, when calculated

22
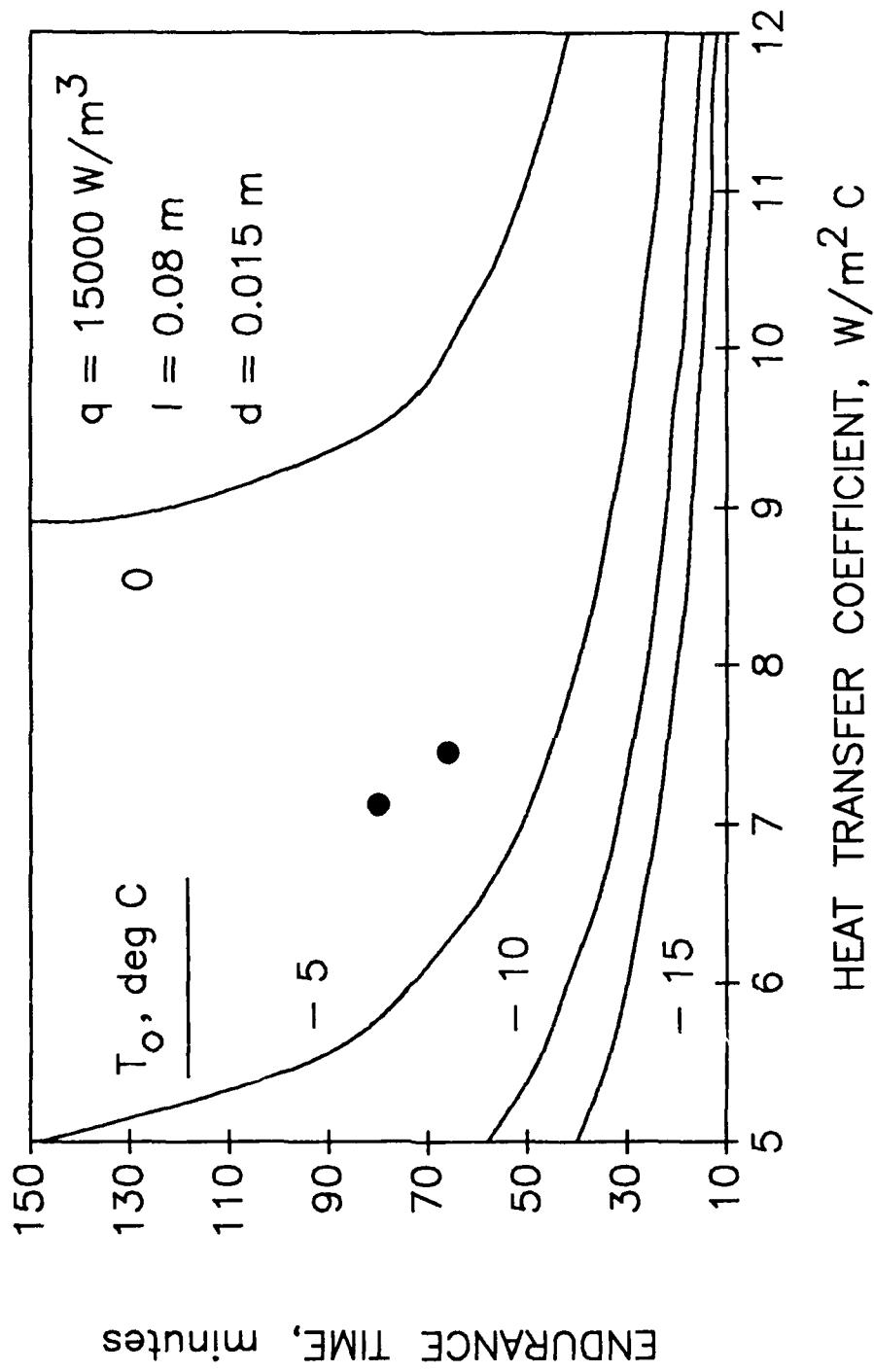
Figure 8. Lower bounds of endurance times for variably insulated fingers exposed to different environmental temperatures. Filled circles indicate average endurance times measured for a -6.7°C environment [11].
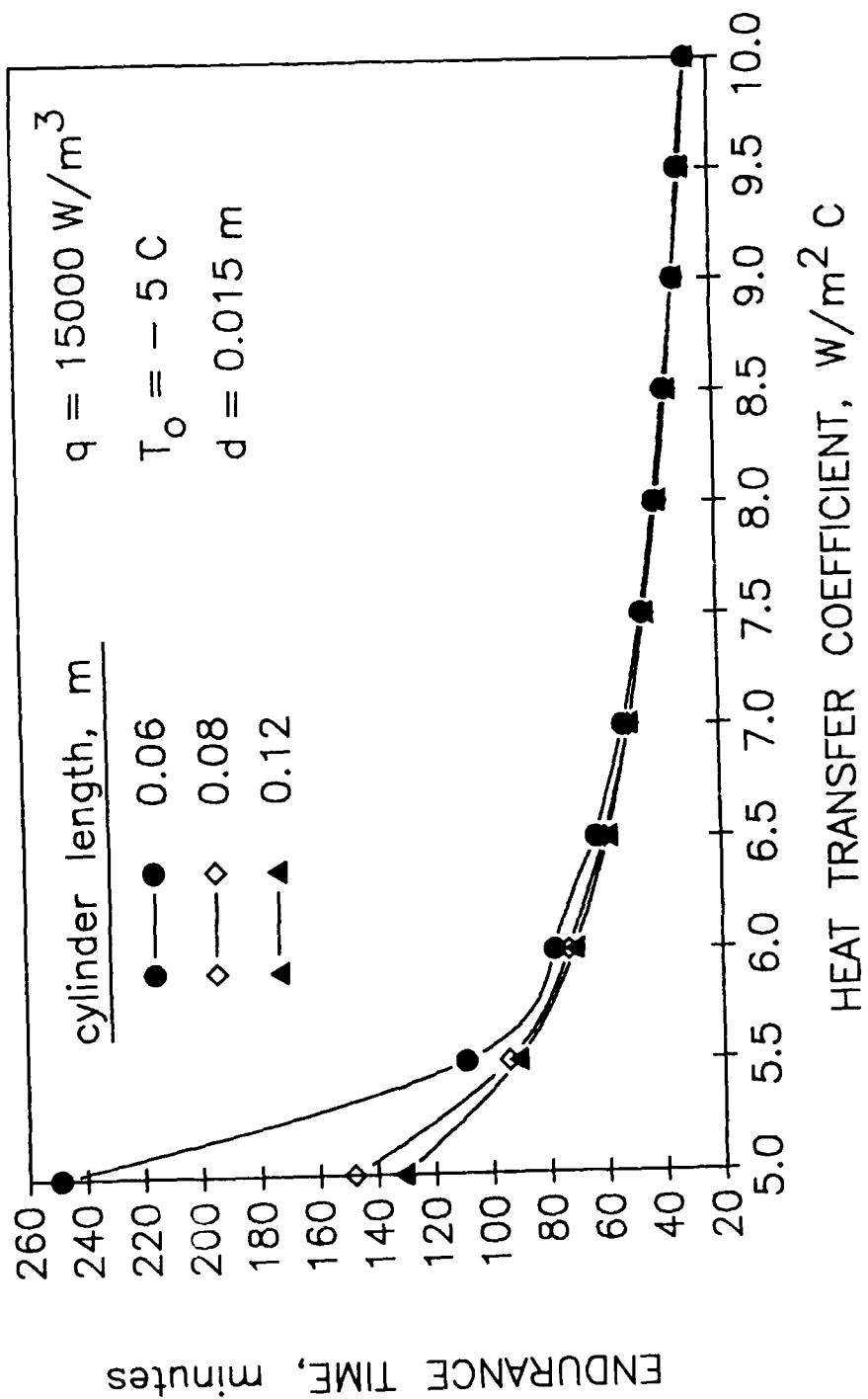
Figure 9. Lower bounds of endurance times for variably insulated fingers of different lengths.
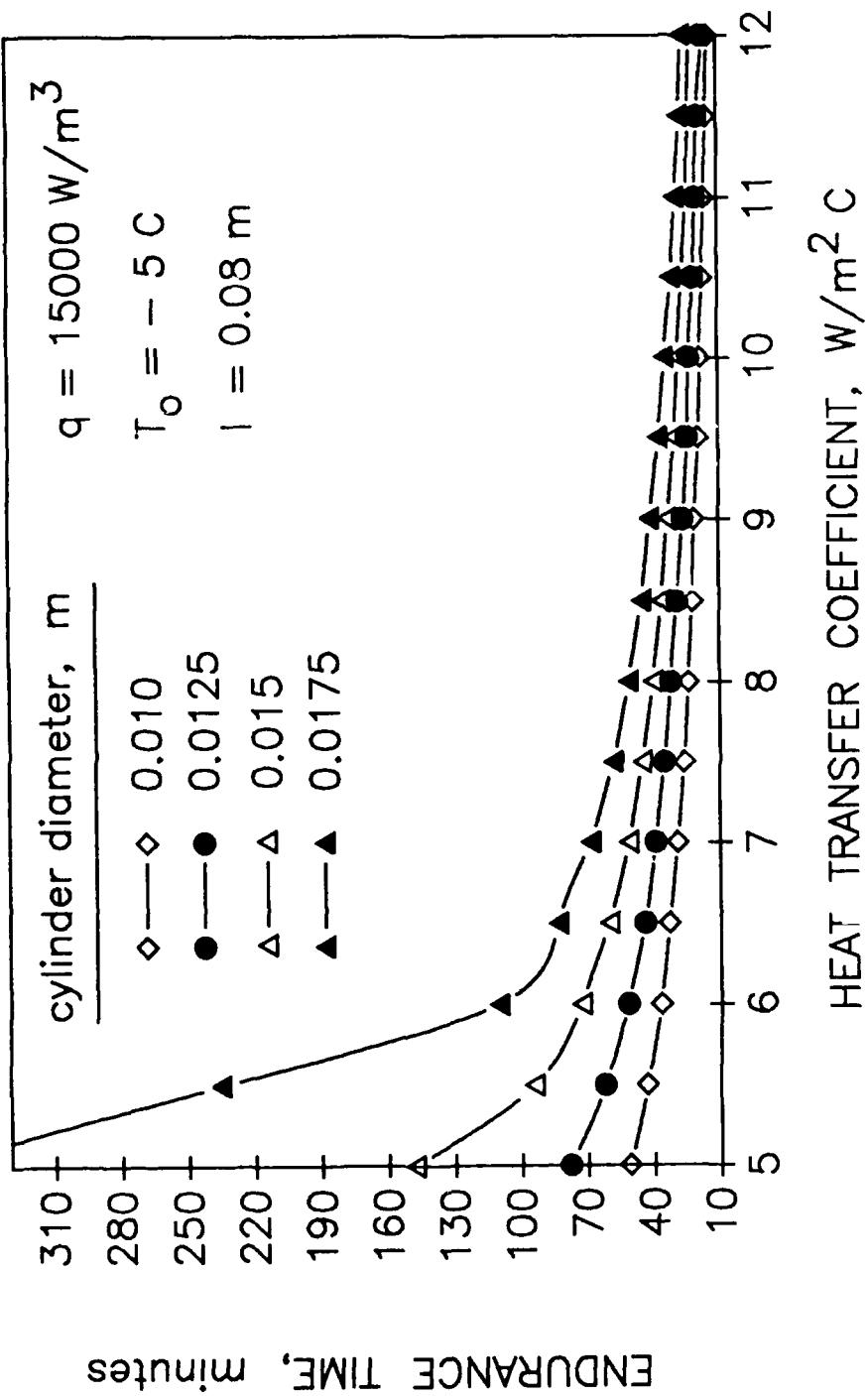
Figure 10. Lower bounds of endurance times for variably insulated fingers of different diameters.

appropriately, would provide conservative estimates of permissible exposure times of fingers in cold environments.

CONCLUSION

The model developed in this study is useful in calculating temperature variations along insulated digits and in predicting their endurance times to cold exposures. Calculated results compared very favorably with data obtained on human subjects. The present version of the model does not include the effect of cold induced vasodilatation. Expansion of the model to include this important natural mechanism will tend, as a general rule, to predict longer, less conservative endurance times. Thus, predictions based on the present model should be useful whenever conservative, lower bounds of endurance times to cold exposures are required.

REFERENCES

1. Goldman, R.F. The Arctic soldier: Possible research solutions for his protection. In: Science in Alaska, Proceedings 15th Alaskan Science Conference, College, Alaska. G. Dahlgren (Ed.), Alaska Division, Assn. for the Advancement of Science, pp. 401-419, 1964.

2. Burton, A.C. Range and variability of blood flow in the human fingers. Am. J. Physiol., 127:437-453, 1939.

3. Van Dilla, M., R. Day and P.A. Siple. Special problems of hands. In: Physiology of Heat Regulation and the Science of Clothing. L.H. Newburgh (Ed.), W.B. Saunders Co., Philadelphia, PA, pp. 374-388, 1949.

4. Molnar, G.W. Analysis of the rate of digital cooling. J. de Physiol., 63(3):350-352, 1971.

5. Wilson, O. and R.F. Goldman. Role of air temperature and wind in the time necessary for a finger to freeze. J. Appl. Physiol. 29(5):658-664, 1970.

6. Wilson, O., R.F. Goldman and G.W. Molnar. Freezing temperature of finger skin. J. Appl. Physiol., 41(4):551-558, 1976.

7. Santee, W.R., T.L. Endrusick and L.P. Wells. Biophysical evaluation of handwear for cold weather use by petroleum (POL) handlers. In: Trends in Ergonomics/Human Factors V. F. Aghazadeh (Ed.), Elsevier Science Publishers B.V. (North Holland), pp. 441-448, 1988.

8. Ozisik, M.N. Heat Transfer - A Basic Approach, McGraw-Hill Book Co., New York, 1985.

9. Shitzer, A. and M.K. Kleiner. Thermal behavior of biological tissues - a general analysis. Bul. Math Bio., 38:369-386, 1976.

10. Dusek, E.R. Manual performance and finger temperatures as a function of ambient

temperature. Headquarters Quartermaster Research and Engineering Research Center for Environmental Protection Research Division. Technical Report No. EP-68, 1957.

11. Santee, W.R., T.L. Endrusick and L.S. Pensotti. Comparison of light duty gloves with natural and synthetic materials under wet and dry conditions. In: <u>Advances in Industrial Ergonomics and Safety</u>, B.Das (Ed.), Taylor and Francis Publishers, Vol. 2, pp. 347-354, 1990.

12. Coffman, J.D. and Cohen, A.S. Total and capillary fingertip blood flow in Raynaud's phenomenon. <u>N. Engl. J. Med.</u>, 285(5):259-263, 1971.

APPENDIX A: DERIVATION OF THE SOLUTION

For convenience, the set of equations to be solved is repeated here:

$$\frac{1}{\alpha}\frac{\partial T}{\partial t} = \frac{\partial^2 T}{\partial z^2} - \frac{4h}{kd}(T - T_o) + \frac{q(t)}{k} \qquad (A.1)$$

where α is thermal diffusivity defined by $\alpha = k/\rho c$.

$$T = T_1(t) \qquad @ \ z = 0, \ t \geq 0 \qquad (A.2)$$

$$-k\frac{\partial T}{\partial z} = h_1(T - T_0) \qquad @ \ z = \ell, \ t \geq 0 \qquad (A.3)$$

$$T = T_i(z) \qquad @ \ t = 0, \ 0 \leq z \leq \ell \qquad (A.4)$$

The following transformation is applied

$$T(z, t) = v(z, t) - f_1(z) F_o(t) + T_o \qquad (A.5)$$

where

$$F_o(t) = T_1(t) - T_o \qquad (A.6)$$

Substitution of Eq. (A.5) into Eqs. (A.1) - (A.4) yields:

$$\frac{1}{\alpha} \left[\frac{\partial v}{\partial t} - f_1(z) \frac{dF_o}{dt} \right] = \frac{\partial^2 v}{\partial z^2} - F_o(t) \frac{d^2 f_1}{dz^2} - \frac{4h}{kD} \left[v - f_1(z) F_o(t) \right] \qquad \text{(A.7)}$$

$$v(0, t) - f_1(0) F_o(t) = F_o(t) \qquad @ \ z = 0 \qquad \text{(A.8)}$$

$$k \left[\frac{\partial v}{\partial z} - F_o(t) \frac{df_1}{dz} \right] + h_1 \left[v - f_1(z) F_o(t) \right] = 0 \qquad @ \ z = \ell \qquad \text{(A.9)}$$

$$v(z, 0) - f_1(z) F_o(0) = T_I(z) - T_o \qquad \text{(A.10)}$$

The function $f_1(z)$ may be chosen to satisfy certain conditions without loss of generality [9]. In the present case, and for the sake of convenience, the following conditions are chosen:

$$\frac{d^2 f_1}{dz^2} = 0 \qquad \text{(A.11)}$$

$$f_1(0) = -1 \qquad \text{(A.12)}$$

$$k \frac{df_1(\ell)}{dz} + h_1 f_1(\ell) = 0 \qquad \text{(A.13)}$$

Solution of Eqs. (A.11) - (A.13) yields

$$f_1(z) = \frac{h_1}{k + h_1 \ell} z - 1 \tag{A.14}$$

An alternative form for $f_1(z)$ would be

$$f_1(z) = \frac{Bi}{1 + Bi} \left(\frac{z}{\ell}\right) - 1 \tag{A.15}$$

where

$$Bi = \frac{h_1 \ell}{k} \tag{A.16}$$

and Bi is the Biot modulus indicating the ratio of convected heat at the cylinder tip to the heat conducted toward the tip inside the cylinder.

Substituting Eq. (A.15) into Eqs. (A.7) - (A.10) and performing the indicated operations yields

$$\frac{1}{\alpha} \frac{\partial v}{\partial t} = \frac{\partial^2 v}{\partial z^2} - Lv + f_1(z) \left[L F_o(t) + \frac{1}{\alpha} \frac{dF_o}{dt} \right] + \frac{q(t)}{k} \tag{A.17}$$

$$v(0, t) = 0 \qquad @ \ z = 0 \tag{A.18}$$

$$k \frac{\partial v}{\partial z} + h_1 v = 0 \qquad @ \ z = \ell \tag{A.19}$$

$$v(z, 0) = T_i(z) - T_o + f_1(z) F_0(0) \qquad @ \ t = 0 \tag{A.20}$$

Inspection of Eqs. (A.17) - (A.20) reveals that both boundary conditions, Eqs. (A.18) and (A.19), are homogeneous. This is the desired result of the application of the above transformation, Eq. (A.5), and the selection of the conditions for $f_1(z)$. One self-suggesting method of solution of Eqs. (A.17) -(A.20), would be by applying an orthogonal transformation to eliminate the dependence on the spatial variable, z. The eigenvalue equation for the problem is obtained from Eq. (A.19).

$$k\beta_n\cos\beta_n + h_1\ell\sin\beta_n = 0 \tag{A.21}$$

or:

$$\beta_n\cot\beta_n = -Bi \tag{A.22}$$

The integral transformation applied to eliminate the spatial variable z, is defined by [8,9]

$$\overline{\Omega}_n(t) = \int_0^\ell \Omega(z,t)K(n,z)\,dz \tag{A.23}$$

where the bar indicates the transformed function which is a function of the remaining variable t only. $K(n,z)$ is the kernel defined by

$$K(n,z) = \frac{1}{N_n}K_n(z) \tag{A.24}$$

where $K_n(z)$ are the eigenfunctions of the auxiliary Sturm-Lioville problem in z [8], given for the present case by

$$K_n(z) = \ell\sin\frac{\beta_n z}{\ell} \tag{A.25}$$

32

and N_n is the normalization integral

$$N_n = \int_0^\ell [K_n(z)]^2 \, dz \tag{A.26}$$

In the present case

$$K(n, z) = \frac{2(\beta_n^2 + Bi^2)}{\ell^2(\beta_n^2 + Bi^2 + Bi)} \sin \frac{\beta_n z}{\ell} \tag{A.27}$$

The transforming equation (A.23) is applied now to Eqs. (A.17) - (A.20). Integration steps would not be repeated here but for the sake of clarity the formal application of the transformation is shown in its entirety:

$$\frac{1}{\alpha} \frac{d}{dt} \int_0^\ell v(z, t) K(n, z) dz = \int_0^\ell \frac{\partial^2 v}{\partial z^2} K(n, z) dz - L \int_0^\ell v K(n, z) dz +$$

$$\frac{q(t)}{k} \int_0^\ell K(n, z) dz + \{LF_o(t) + \frac{1}{\alpha} \frac{dF_o}{dt}\} \cdot \int_o^\ell f_1(z) K(n, z) dz \tag{A.28}$$

Both boundary conditions, Eqs. (A.18) and (A.19), are satisfied by the set of eigenfunctions. The initial condition, Eq. (A.20) is transformed by applying Eq. (A.23) to yield

$$\int_0^\ell v(z, 0) K(n, z) dz = \int_0^\ell \{T_i(z) - T_o + f_1(z) F_o(0)\} K(n, z) dz \tag{A.29}$$

Performing the indicated integrations and rearranging terms, yields an ordinary differential equation of the transformed function $\bar{v}(t)$:

33

$$\frac{d\bar{v}}{dt} + \alpha \lambda_n^2 \bar{v} = -\alpha G(t) \tag{A.30}$$

subject to the transformed initial condition

$$\bar{v}(0) = \tau \qquad @ \ t = 0 \tag{A.31}$$

where

$$\lambda_n^2 = \left(\frac{\beta_n}{\ell}\right)^2 + L \tag{A.32}$$

$$G(t) = \frac{B_n \ell}{\beta_n}\{LF_o(t) + \frac{1}{\alpha}\frac{dF_o}{dt}\} + \frac{q(t)\ell B_n}{k\beta_n}(\cos\beta_n - 1) \tag{A.33}$$

$$B_n = \frac{2(\beta_n^2 + Bi^2)}{\ell^2(\beta_n^2 + Bi^2 + Bi)} \tag{A.34}$$

and

$$\tau = B_n \int_0^\ell [T(z) - T_o] \sin\frac{\beta_n z}{\ell} \, dz - \frac{B_n \ell}{\beta_n} F_o(0) \tag{A.35}$$

The solution of Eq. (A.30), subject to Eq. (A.31), is straightforward and is given by

$$\bar{v}(t) \;=\; \{\tau \,-\, \alpha \int_{\eta=0}^{t} G(\eta)\exp(\alpha\lambda^2\eta)\,d\eta\} \exp(-\alpha\lambda^2 t) \tag{A.36}$$

Inversion of the transformed function, $\bar{v}(t)$, is achieved by employing the orthogonality property of the eigenfunctions. This inversion is performed by

$$v(z,t) \;=\; \sum_{n=1}^{\infty} \bar{v}(t) K_n(z) \tag{A.37}$$

$$v(z,t) \;=\; \ell \sum_{n=1}^{\infty} \{\tau \,-\, \alpha \int_{0}^{t} G(\eta)\exp(\alpha\lambda^2\eta)\,d\eta\} \exp(-\alpha\lambda^2 t)\sin\frac{\beta_n}{\ell} \tag{A.38}$$

The solution for the temperature T(z,t) is obtained by substituting Eq. (A.38) into Eq. (A.5), to yield

$$T(z,t) \;=\; \ell \sum_{n=1}^{\infty} \{\tau \,-\, \alpha \int_{c}^{t} G(\eta)\exp(\alpha\lambda^2\eta)\,d\eta\} \exp(-\lambda^2\alpha t)\sin\frac{\beta_n z}{\ell}$$

$$+\; T_o \,-\, f_1(z)[T_1(t) \,-\, T_o] \tag{A.39}$$

Equation (A.39) is the solution for the original set of equations (A.1) - (A.4).

APPENDIX B: COMPUTER PROGRAM PRINTOUT AND SAMPLE OUTPUT

```
PROGRAM TEMP4; { Calculation of the time-dependent temperature field
                in a cylinder in the axial direction for variable (exponential)
                temperature at z=0 and variable (exponential) heat generation.
                Program written in Turbo-Pascal Version 5.5 }
                { Current version employs time in hours }

uses crt,printer;
LABEL
      30,40,50,
      100,200,300,400,600;
CONST                       { definition of parameters }
      p=3.14159265;
      k=0.418;   { thermal conductivity, W/m/C }
      h=2.0;     { heat transfer coefficient on circumference, W/m^2/C }
      h1=2.0;    { heat transfer coefficient on tip, W/m^2/C }
      D=0.02;    { cylinder diameter, m }
      qi=2000.;  { initial heat generation (metabolic) rate, W/m^3 }
      qf=200;    { final heat generation (metabolic) rate, W/m^3 }
      T0=-5.0;   { environmental temperature, C }
      T1=30.;    { constant base temperature, C }
      T2=30.0;   { base temperature, linear distribution, C }
      T3=20.0;   { tip temperature, linear distribution, C }
      l=0.12;    { cylinder length, m }
      M=40;      { number of terms in series (maximum) }
      ALF=0.0004546; { thermal diffusivity, m^2/hr }
      delta=1.3; { time constant for base temperature, hr }
      Tfin=20.0; { final base temperature, C }
      Tinit=30.0;{ initial base temperature, C }
      eps=1.3;   { time constant for metabolic heat rate, hr }
      KK=11;     { number of time steps in minutes }
TYPE


      vec=ARRAY[1..40] OF double;
      mat=ARRAY[1..20,1..41] OF double;
VAR
  ft,ct                 :text;
  Tfile,cfile           :string;
  init,uniform,linear     :string;
  I,J,N                 :integer;
  T                     :mat;
  Bn,Gn,Hn                :vec;
```

```pascal
    Cn,LAMSn,TAUn,COEFn,b     :vec;
    TIME,temp,Tmax            :double;
    Bi,con,asum,ax            :double;
    x,c,LI,y              :double;
    del,ddx,dev,u,uu,dx       :double;
    q,qq,f,g,A,tot            :double;
    z,ff1,SUM,SUM1,SU,fsin    :double;
FUNCTION Par(y,c:double):double;
  begin
    Par:=y*COS(y)/SIN(y)+c
  end;
FUNCTION Der(y:double):double;
  begin
    Der:=COS(y)/SIN(y)-y*(1.-sqr(COS(y)/SIN(y)))
  end;
FUNCTION F1(y:double):double;
  begin
    F1:=Bi/(1.+Bi)*(y/l)-1.
  end;
BEGIN                { begin execution of main program }
ClrScr;
init:='linear';
                { Nullify initial values of vectors }
FOR n:=1 TO 40 DO
  BEGIN
    Bn[n] :=0.;
    Cn[n]:=0.;
    LAMSn[n]:=0.;
    TAUn[n]:=0.;
    COEFn[n]:=0.;
    b[n]:=0.;
    Gn[n]:=0.;
    Hn[n]:=0.
  END;
WRITELN('k= ',k:6:2,'    h=',h:6:2, '   h1=',h1:6:2,'  ALF=',ALF:16:8) ;
WRITELN('qi= ',qi:6:2,'   qf=',qf:6,'   T0=',T0:6:2);
WRITELN('T1= ',T1:6:2,'   T2= ',T2:6:2,'   T3=',T3:6:2) ;
WRITELN('l= ',l:6:2,'  D=',D:6:2) ;


                { Procedure to calculate the eigenvalues of:
                        f(x)=x*cot(x)+c }


Bi:=h1*l/k;       { Biot modulus }
LI:=4.*h/k/D;
c:=Bi;
WRITELN('Biot=',c:6:2) ;
```

37

```
WRITELN  ;
{ Check values of the parameter c and set initial guesses and increments }
IF c<1.37
THEN     GOTO 50
ELSE
begin
x:=2.2;
ddx:=2.;
del:=0.0001*c
end;
IF c>=1.37 THEN
  begin
    x:=2.1;
    ddx:=2.
  end  ;
IF c>=50. THEN
  begin
    x:=2.7;
    ddx:=3.
  end;
IF c>=200. THEN
  begin
    x:=3.;
    ddx:=3.1
  end;
IF c>=2000. THEN
  begin
    x:=3. ;
    ddx:=3.14
  end ;

          { calculate the first iterative values  }

FOR i:=1 TO M DO
  BEGIN
   dev:=1. ;
30:  u:=1. ;
   uu:=1.  ;
   dx:=0.01/dev;
     WHILE (u*uu)>0 DO
       begin
         x:=x+dx;
     u:=Par(x,c) ;
     uu:=Par(x+dx,c)
       end ;
IF ABS(u)<del THEN
ELSE
```

```
      begin
        dev:=dev*100. ;
    IF dev>1E08 THEN GOTO 600;
        GOTO 30
      end ;
    600: b[i]:=x ;
    x:=x+ddx
    END ;
    GOTO 40 ;

              { Calculate approximate values of roots by using the
                       slope of cot(x) at (2*n-1)*p/2 }


    50:  FOR n:=1 TO M  DO      { calculation for low values of c }
      BEGIN
    IF (n=1) AND (c<(0.5-1)) THEN
    b[1]:=0.1
    ELSE
    {     This portion calculates the eigenvalues for low and negative values
                       of the variable               }
        begin
          q:=(2*n-1)*pi/2 ;
          qq:=q*q+4.*c      ;
          b[n]:=(q+SQRT(qq))/2.
        end
      END;
                    { Start Newton's procedure }

        FOR i:=1 TO M DO
        BEGIN
        f:=1. ;
        x:=b[i] ;
        del:=0.0001*EXP(INT(0.1*i)*LN(10)) ;
        WHILE ABS(f)>del DO
         begin
        f:=Par(x,c)    ;
        g:=Der(x)    ;
        x:=x-f/g
         end ;
      b[i]:=x+f/g
      END;
    40: {FOR l:=1 TO M DO
    WRITEln(l,b[l],Par(b[l],c));}

        {     End of procedure for calculating eigenvalues     }

    FOR l:=1 TO M DO
```

```
BEGIN            { calculation of parameters in series solution }
   A:=b[I]*b[I]+Bi*Bi;
Bn[I]:=2*A/(I*I*(A+Bi))  ;
Cn[I]:=Bn[I]*I/b[I]*(qf*(COS(b[I])-1.0)/k+LI*(Tfin-T0))  ;
LAMSn[I]:=b[I]*b[I]/I/I+LI                           ;
TAUn[I]:=Bn[I]*I/b[I]*((T3-T2)*SIN(b[I])/b[I]+(T2-Tinit)-(T3-T0)*COS(b[I]));
COEFn[I]:=Cn[I]+LAMSn[I]*TAUn[I];
Gn[I]:=Bn[I]*I/b[I]*LAMSn[I]*(Tinit-Tfin)*(ALF*DELTA*LI-1.0)/(ALF*LAMSn[I]*
      DELTA-1.0);
Hn[I]:=ALF*I*Bn[I]/k/b[I]*(COS(b[I])-1.0)*LAMSn[I]*(qi-qf)*eps/
      (eps*ALF*LAMSn[I]-1.0)
END;
                   { estimation of time to reach steady state }

Tmax:=LN(abs(1000*(COEFn[1]+Gn[1]+Hn[1])/Cn[1]))/(ALF*LAMSn[1]);
WRITELN(' Tmax=',Tmax:10:5,' hr','  T0=',T0:10:5,' deg C');

Tfile := 'Test.dat';   { open output file }
assign(ft,Tfile);
rewrite(ft);
WRITELN(ft,'k= ',k:6:2,'     h=',h:6:2, '   h1=',h1:6:2,'  ALF=',ALF:16:8) ;
WRITELN(ft,'qi= ',qi:6:2,'   qf=',qf:6,'    T0=',T0:6:2);
WRITELN(ft,'T1= ',T1:6:2,'   T2= ',T2:6:2,'   T3=',T3:6:2)  ;
WRITELN(ft,'l= ',l:6:2,'  D=',D:6:2)  ;
WRITELN(ft,'Biot=',c:6:2)  ;
WRITELN(ft);
 FOR i:=1 TO KK  DO    { time steps }
 begin
 write(ft,i-1:2,'   ');
    TIME:=(i-1);
      IF TIME=0. THEN
        TIME:=0.00001
      ELSE;
      if i=KK then TIME:=Tmax
      else  ;
FOR j:=1 TO 11   DO
BEGIN
  z:=(j-1)*l/10. ;
  ff1:=F1(z)    ;
 SUM:=0.        ;
 con:=1.  ;
 N:=1 ;
 WHILE ((N<(M+1)) AND (con>asum)) DO
    begin  {while}
    SUM1:=SUM  ;
    IF (abs(ALF*LAMSn[N]*TIME)>LN(abs(1000*(COEFn[N]+Gn[N]+Hn[n])
                              /Cn[N]))) THEN
```

40

```
          SUM:=SUM-(Cn[N]+Gn[N]*EXP(-TIME/DELTA)+Hn[N]*EXP(-TIME/eps))*
              SIN(b[N]*z/l)/LAMSn[N]
      ELSE
    SUM:=SUM+((COEFn[N]+Gn[N]+Hn[N])*EXP(-ALF*LAMSn[N]*TIME)-Cn[N]-Gn[N]*
              EXP(-TIME/DELTA)-Hn[N]*EXP(-TIME/eps))*SIN(b[N]*z/l)/LAMSn[N];
      con:=abs(ABS(SUM)-ABS(SUM1)) ;
      asum:=0.001*ABS(SUM) ;
      N:=N+1
    end ;   {while}
200: {WRITE(z,N,SUM);}
TEMP:=l*SUM+T0-ff1*(Tfin+(Tinit-Tfin)*EXP(-TIME/DELTA)-T0) ;
T[j,i]:=TEMP;
write(ft, temp:6:4,' ');
END ;
writeln(ft);
end;                 { end time steps }
close(ft);
tot:=0.;
for i:=1 to KK  do       { time steps }
begin
write(i-1:2);
for j:=1 to 11 do        { space steps }
begin
write(T[j,i]:7:3);
tot:=tot+T[j,i]   { sum of all printed values; used to check consistency }
end;
writeln
end;   { end printing of temperature matrix  }
writeln(' total=',tot:10:5) ;

100: END.
```

Sample output of PROGRAM TEMP4

k= 0.42
qi= 2000.00
T1= 30.00
l= 0.12
Biot= 0.57

h= 2.00
qf= 200
T2= 30.00
D= 0.02

h1= 2.00
T0= -5.00
T3= 20.00

ALF= 0.00045460

0	29.9999	29.0000	28.0001	26.9986	26.0057	25.0002	23.9964	23.0105	21.9801	20.9902	19.9535
1	24.6337	20.9031	18.7536	17.4206	16.4509	15.7120	15.0053	14.2995	13.5575	12.7364	11.8242
2	22.1471	16.9094	13.7155	11.6643	10.3123	9.4324	8.7332	8.1520	7.5791	6.9854	6.3621
3	20.9949	14.8077	10.8793	8.2553	6.5542	5.4677	4.6661	4.0875	3.5893	3.1330	2.6931
4	20.4610	13.6906	9.2822	6.3495	4.2984	3.0256	2.1167	1.5006	1.0227	0.6368	0.3036
5	20.2136	13.0915	8.3826	5.2034	2.9594	1.5393	0.5519	-0.1065	-0.5860	-0.9442	-1.1998
6	20.0990	12.7681	7.8759	4.5414	2.1716	0.6572	-0.3947	-1.0887	-1.5765	-1.9174	-2.1313
7	20.0459	12.5907	7.5871	4.1565	1.7075	0.1322	-0.9623	-1.6809	-2.1761	-2.5079	-2.6969
8	20.0213	12.4932	7.4231	3.9342	1.4363	-0.1775	-1.2998	-2.0351	-2.5363	-2.8637	-3.0380
9	20.0098	12.4391	7.3296	3.8057	1.2780	-0.3596	-1.4993	-2.2455	-2.7510	-3.0761	-3.2419
10	20.0002	12.3730	7.2106	3.6390	1.0699	-0.6014	-1.7664	-2.5289	-3.0415	-3.3643	-3.5076

42

GLOSSARY

A	- cross sectional area
Bi	- Biot modulus, Eq. (A.16)
B_n	- parameter, Eq. (7)
c	- specific heat
C_n	- parameter, Eq. (18)
d	- diameter
f_1	- function, Eq. (10)
F_o	- function, Eq. (9)
G	- defined by Eq. (8)
G_n	- parameter, Eq. (19)
h	- heat transfer coefficient at cylinder circumference
h_1	- heat transfer coefficient at cylinder tip
H_n	- eigenfunction, Eq. (A.25)
k	- thermal conductivity
K	- kernel, Eg. (A.24)
K_n	- eigenfunction, Eq. (A.25)
l	- cylinder length
L	- 4h/kd
n	- integer
N_n	- normalization integral, Eq. (A.26)
p	- cylinder circumference

q   - metabolic heat generation rate per unit volume

t   - time

T   - temperature

T_2, T_3 - temperatures in linear initial distribution, Eq. (13)

v   - function, Eq. (A.5)

z   - axial coordinate

GREEK LETTERS

α - k/ρc, thermal diffusivity

β_n - eigenvalue, Eq. (11)

δ - time constant for cylinder base temperature, Eq. (15)

ϵ - time constant for metabolic *heat generation rate*, Eq. (16)

ζ - integration variable, Eq. (12)

η - integration variable, Eq. (5)

λ_n^2 - parameter, Eq. (A.32)

ρ - density

τ - defined by Eq. (6)

Ω - function

$\bar{\Omega}_n$ - transformed function, Eq. (A.23)

SUBSCRIPTS

o   - environmental

1   - cylinder base

f   - final

i   - initial

SUPERSCRIPTS

-        - transformed function, defined by Eq. (A.23)

*   - steady state

DISTRIBUTION LIST

2 Copies to:

Commander
U.S. Army Medical Research and Development Command
ATTN: SGRD-OP
Fort Detrick
Frederick, MD 21701-5012

Commander
U.S. Army Medical Research and Development Command
ATTN: SGRD-PLE
Fort Detrick
Frederick, MD 20701-5012

Commander
U.S. Army Medical Research and Development Command
ATTN: SGRD-PLC
Fort Detrick
Frederick, MD 20701-5012

1 Copy to:

Commandant
Academy of Health Sciences, U.S. Army
ATTN: AHS-COM
Fort Sam Houston, TX 78234-6100

Stimson Library
Academy of Health Sciences, U.S. Army
ATTN: Chief Librarian
Bldg. 2840, Room 106
Fort Sam Houston, TX 78234-6100

Director, Biological Sciences Division
Office of Naval Research - Code 141
800 N. Quincy Street
Arlington, VA 22217

Commanding Officer
Naval Medical Research and Development Command
NMC-NMR/ Bldg. 1
Bethesda, MD 20814-5044

Office of Undersecretary of Defense for Acquisition
ATTN: Director, Defense Research and Engineering
    Deputy Undersecretary for Research & Advanced Technology
    (Environmental and Life Sciences)
    Pentagon, Rm. 3D129
    Washington D.C. 20301-3100

Dean
School of Medicine
Uniformed Services University Of The Health Sciences
4301 Jones Bridge Road
Bethesda, MD 20814-4799

2 Copies to:

Commander
U.S. Army Medical Research Institute of Chemical Defense
Aberdeen Proving Ground, MD 21010-5425

Commander
U.S. Army Chemical Research, Development and Engineering Center
Aberdeen Proving Ground, MD 21010-5423

Commandant
U.S. Army Chemical School
Fort McClellan, AL 36205-5020

Commander
U.S. Air Force School of Aerospace Medicine
Brooks Air Force Base, TX 78235-5000

Commander
Naval Health Research Center
P.O. Box 85122
San Diego, CA 92138-9174

Commander
U.S. Army Biomedical Research and Development Laboratory
Fort Detrick
Frederick, MD 21701-5010

Commander
U.S. Army Medical Materiel Development Activity
Fort Detrick
Frederick, MD 21701-5009

U.S. Army Scientific Liaison Officer to DCIEM
(U.S. Army Medical R&D Command)
1133 Sheppard Avenue W.
P.O. Box 2000
Downsview, Ontario
CANADA M3M 3B9

1 Copy:

Commandant
Walter Reed Army Institute of Research
Walter Reed Army Medical Center
ATTN: SGRD-UWZ-C (Director for Research Management)
Washington D.C. 20307-5100

Commander
U.S. Army Environmental Hygiene Agency
Aberdeen Proving Ground, MD 21010-5422